

Communication

Synthesis and In Vitro Antibacterial Evaluation of Mannich Base Nitrothiazole Derivatives

Phelisiwe S. Dube ^{1,*}, Dylan Hart ¹, Lesetja J. Legoabe ¹, Audrey Jordaan ², Digby F. Warner ^{2,3,4}
and Richard M. Beteck ¹

¹ Centre of Excellence for Pharmaceutical Sciences, North-West University, Potchefstroom 2520, South Africa; lesetja.legoabe@nwu.ac.za (L.J.L.); richmbi1@yahoo.com (R.M.B.)

² SAMRC/NHLS/UCT Molecular Mycobacteriology Research Unit, Department of Pathology, University of Cape Town, Observatory 7925, South Africa

³ Institute of Infectious Disease and Molecular Medicine, University of Cape Town, Rondebosch 7701, South Africa

⁴ Welcome Centre for Infectious Diseases Research in Africa (CIDRI-Africa), Faculty of Health Sciences, University of Cape Town, Rondebosch 7701, South Africa

* Correspondence: 29683130@mynwu.ac.za or phelelisiwedube@gmail.com; Tel.: +27-182992249

Abstract: Nitrothiazole derivatives have been reported to exhibit activity against aerobic, anaerobic, and microaerophilic bacteria. This activity profile makes the nitrothiazole compound class an ideal lead source against *Mycobacterium tuberculosis*, which flourishes in varied environments with different oxygen concentrations. In this work, we investigated six nitrothiazole derivatives for antitubercular activity. The compounds exhibited potent activity, with compounds **9** and **10** possessing an equipotent MIC₉₀ value of 0.24 µM. The compounds were investigated for cytotoxicity against HEK293 cells and hemolysis against red blood cells, and they demonstrated no cytotoxicity nor hemolytic effects, suggesting they possess inherent antitubercular activity.

Keywords: nitrothiazole; Mannich bases; antitubercular activity; tuberculosis; *Mycobacterium tuberculosis*



Citation: Dube, P.S.; Hart, D.; Legoabe, L.J.; Jordaan, A.; Warner, D.F.; Beteck, R.M. Synthesis and In Vitro Antibacterial Evaluation of Mannich Base Nitrothiazole Derivatives. *Molbank* **2024**, *2024*, M1793. <https://doi.org/10.3390/M1793>

Academic Editors: Antonio Salomone and Serena Perrone

Received: 22 February 2024

Revised: 5 March 2024

Accepted: 11 March 2024

Published: 18 March 2024



Copyright: © 2024 by the authors. Licensee MDPI, Basel, Switzerland. This article is an open access article distributed under the terms and conditions of the Creative Commons Attribution (CC BY) license (<https://creativecommons.org/licenses/by/4.0/>).

1. Introduction

Tuberculosis (TB), primarily caused by *Mycobacterium tuberculosis* (Mtb) [1], is a lethal infection that affects people all over the world [2]. Although Mtb was discovered in 1882 by Robert Koch [3], it is still a serious public health threat today, with about 2 million human lives lost each year to TB and roughly two billion people latently infected with the bacterium [4]. Mtb can exist in the replicative and dormant states [5]. The dormant state, which causes a latent infection, is characterized by low metabolic activity, phenotypic drug resistance, and slow growth [6]. A competent immune system ensures this dormancy. However, when the immune system is compromised or weakened, latent infection can evolve into active disease [7].

Approximately 10 million new cases of active TB are reported annually [8]. Some of these cases result from the reactivation of latent Mtb infection [9]. Factors promoting the reactivation of latent infection include immune-compromising conditions such as diabetes and infection with human immunodeficiency virus/acquired immunodeficiency syndrome (HIV/AIDS) [10]. These factors are prevalent in TB endemic areas [10].

Nitrothiazole derivatives tizoxanide (TIZ) and nitazoxanide (NTZ) (Figure 1) have been reported to enhance immune clearance of dormant Mtb by stimulating autophagy [2]. NTZ inhibits the enzymatic activity of NADPH quinone oxidoreductase (NQO1), leading to the stimulation of autophagy [11]. With regard to Mtb, NTZ kills bacilli (dormant and replicating) through the disruption of membrane potential and pH homeostasis [12]. NTZ is one of the seven repurposed drugs presently being evaluated in phase II clinical studies for the potential treatment of TB [13]. Moreover, it has been proposed that new treatments

that inhibit Mtb in the dormant state can simplify and/or shorten TB treatment; hence, nitrothiazole derivatives have the potential to shorten TB treatment [14,15].

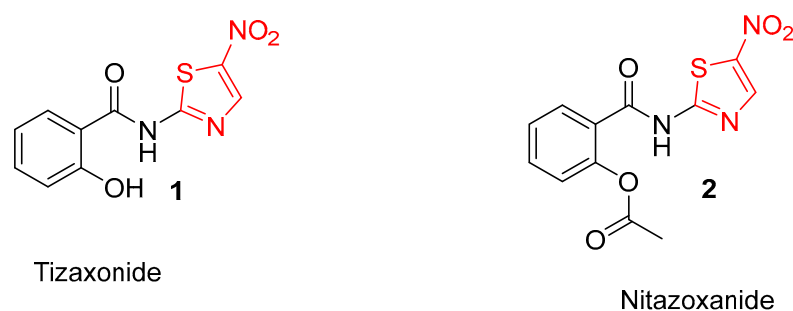


Figure 1. Nitrothiazole derivatives with antitubercular activity.

Nitrothiazole-based compounds seem to have a mode of action against Mtb which is different from that exhibited by current TB agents [16]. Moreover, nitrothiazole derivatives have not been extensively explored, and as such, they present a potential source of novel antitubercular agents [17]. To this effect, we herein propose the synthesis of novel nitrothiazole derivatives and investigate their antitubercular properties.

In this study, we synthesized Mannich base nitrothiazole derivatives and evaluated them *in vitro* for inhibitory activities against six bacteria (*Mtb*, *Staphylococcus aureus*, *Escherichia coli*, *Klebsiella pneumoniae*, *Acinetobacter baumannii*, *Pseudomonas aeruginosa*), and two fungi (*Candida albicans*, and *Cryptococcus neoformans*). These compounds were also evaluated for potential toxicity against the human embryonic kidney cell line (HEK293). Generally, these compounds showed inhibitory activity against Mtb only. They were inactive against fungi and the other bacteria deployed, and showed no toxic potential against HEK293.

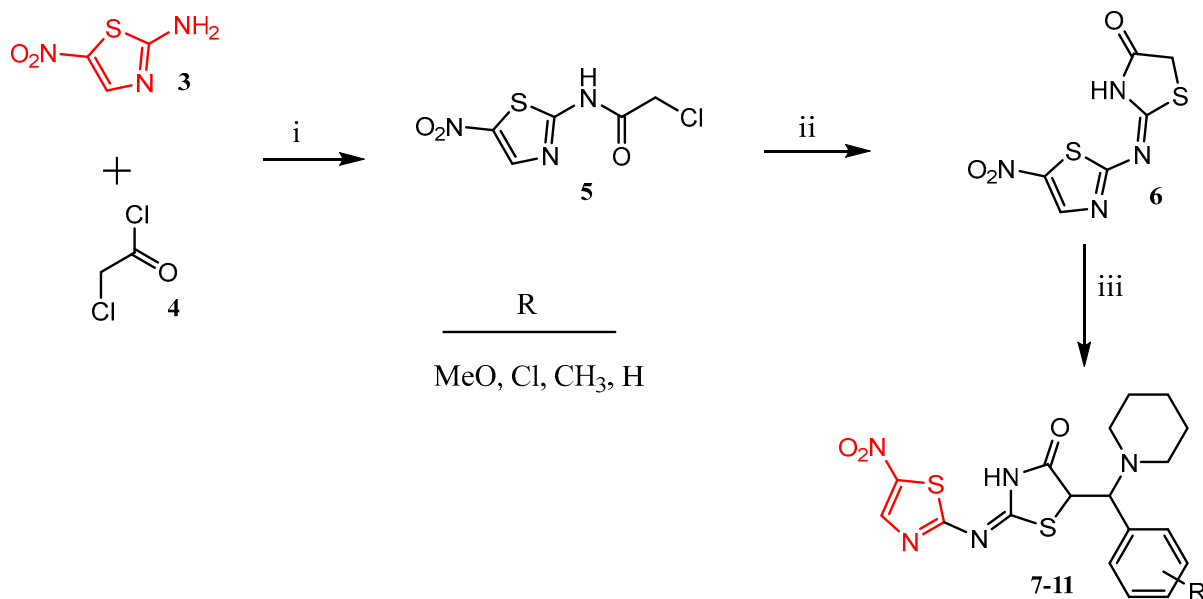
2. Results and Discussion

2.1. Results

Chemistry

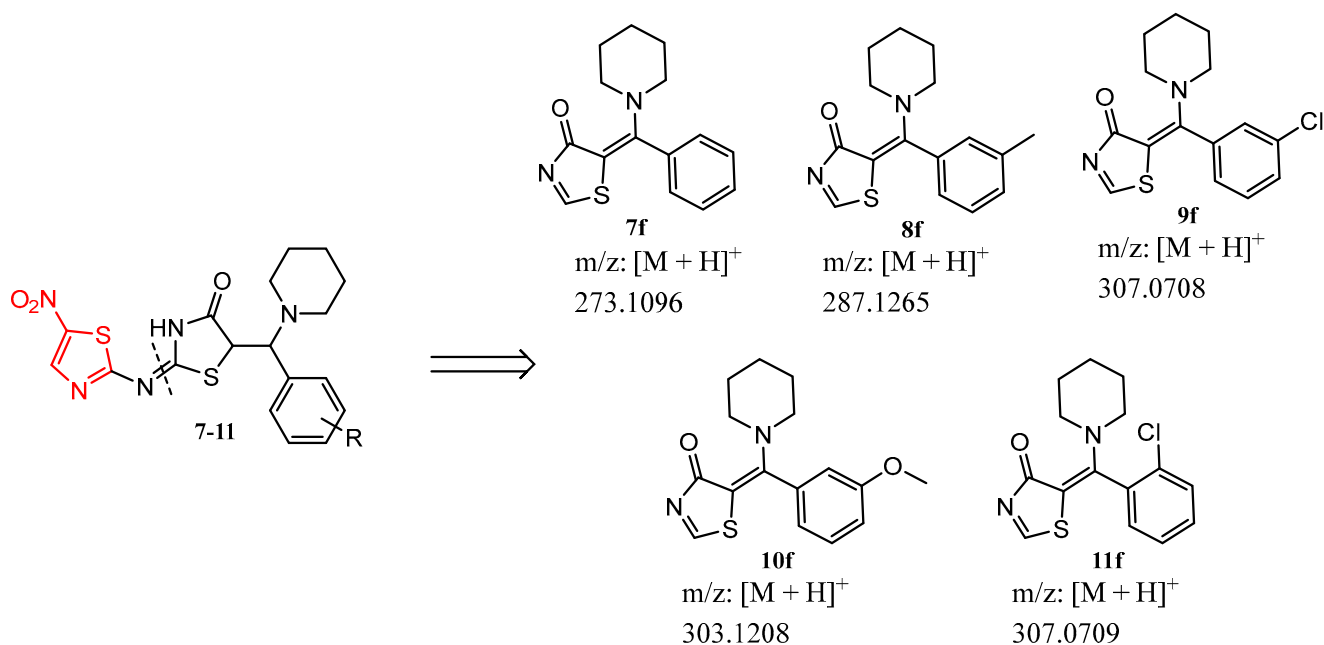
The target compounds were obtained through a multi-step synthetic route represented in Scheme 1. The first step was *N*-acylation of the 2-amino-5-nitrothiazole with 2-chloroacetyl chloride to afford **5**, followed by concurrent *S*-alkylation and intramolecular cyclization to obtain intermediate **6**. Then, treatment of **6** with piperidine and assorted benzaldehydes furnished the Mannich base compounds **7–10**. Reactions were monitored using thin layer chromatography (TLC), and the synthesized compounds were characterized using proton (^1H), carbon (^{13}C), nuclear magnetic resonance (NMR) spectroscopy, and high-resolution mass spectrometry (HRMS). On the ^1H NMR spectra, the signals of the respective protons of the prepared derivatives were verified based on their chemical shifts, multiplicities, and coupling constants. The signals appearing at ca 1.5–2.5 ppm of all the compounds were assignable to the 10 protons of the piperidinyl ring. The peaks at ca 3.6–4.9 ppm were indicative of protons attached to the two chiral carbons, which was also proof of the successful Mannich base condensation reaction. The signals at ca 6.5–7.0 ppm were assignable to the protons of the benzyl ring. In addition, the signal appearing around 7.05–8.0 ppm could be attributed to the proton of the nitrothiazole ring.

For ^{13}C NMR spectra, the signals at ca 20–40 ppm were assignable to the carbons of the piperidinyl ring. The signal around 50 ppm was assigned to the sp^3 carbon of the thiazolidone ring. The signal at ca 49 ppm was assigned to the chiral *N*-methanetriyl carbon linking all three rings (thiazolidone, piperidine, and the benzyl ring). In addition, the signal at ca 120–140 ppm was indicative of the carbons of the benzyl ring. The carbons of the nitrothiazole ring were indicated by the signals at ca 140–150 ppm. Lastly, the peak ca 180 ppm was indicative of the sp^2 carbonyl carbon ($\text{C}=\text{O}$) of the thiazolidinone ring.



Scheme 1. Synthesis of Nitrothiazole-Mannich base derivatives. **Reagents and conditions:** (i) DCM, TEA, 0 °C, 24–36 h; (ii) NH₄SCN, EtOH, reflux, 4–8 h; (iii) piperidine (5 eq), aldehyde (5 eq), EtOH, reflux, 24–36 h.

HRMS analyses did not confirm the expected molecular ions for all compounds, but showed a fragmentation pattern that was consistent for all compounds. We deduced that the fragmentation led to the elimination of the 2-imino-5-nitrothiazolyl moiety, which subsequently deprotonated the amide and active methylene units, followed by re-arrangement to generate the structures depicted in Scheme 2. The consistent mass difference was 144 Da, and this corresponded to the molecular weight of 2-amino-5-nitrothiazole. The predicted molecular formulae during HRMS analyses showed a 100% score with the formulae of the proposed structures in Scheme 2.



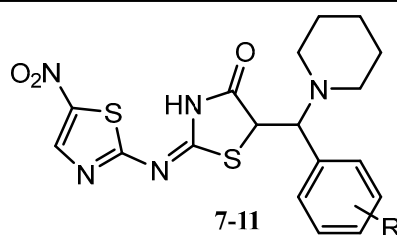
Scheme 2. Structures of fragments formed during ionization.

2.2. Discussion

In Vitro Anti-Tubercular Activity and Calculated Drug-like Properties

Compounds **7–11** were screened in vitro for anti-tubercular activity against the gfp reporter strain of Mtb using supplemented middlebrook 7H9 broth media culture. Rifampicin, a first-line anti-tubercular agent, was included in the assay as a reference. The anti-tubercular activity, presented as the minimum concentration required to inhibit 90% (MIC₉₀) of the bacteria population, was determined on day 14 following the incubation of Mtb in media culture with target compounds. The anti-tubercular activity data are summarized in Table 1. Four compounds were active against Mtb, exhibiting activity in the range of 0.244–31.25 μM. Compounds **9** and **10**, exhibited sub micromolar activity of <0.244 μM. Thus, they were the most active compounds for this compound class.

Table 1. In vitro anti-tubercular activity, ClogP, and structure of target compounds.



Entry	WM/Da	tPSA	^a ClogP	R	HEK293	MIC ₉₀ (μM) vs. Mtb on Day 14
					CC ₅₀ (μM)	CAS, GLU, TX
7	417	108	1.1	H	32	31.25
8	431	108	1.6	<i>m</i> -CH ₃	32	3.795
9	451	108	1.8	<i>m</i> -Cl	32	<0.244
10	447	118	1.0	<i>m</i> -MeO	32	<0.244
11	451	108	1.8	<i>o</i> -Cl	32	125
RF	-	-	-	-	-	0.01

^a clog *p* values calculated with chem draw professionals. RF = rifampicin. CAS = casitone, GLU = glucose, TX = tyloxapol.

Different substituents, although limited, were appended on the phenyl ring to establish how activity varied with modifications at this part of the molecule. The activity seemed to be influenced by the nature of the phenyl substituents. The structure–activity relationship (SAR) showed that substitution of the phenyl ring at the meta position generally led to an increase in anti-tubercular activity, with chlorine and methoxy moieties being the most favored. This is evident when looking at compounds **9** and **10**, both exhibiting sub-micromolar activity of <0.244 μM. In addition, the presence of a methyl moiety attached to the phenyl ring also promoted anti-tubercular activity more effectively than the unsubstituted ring. This is evident when looking at compound **8**, which exhibited activity of 3.795 μM. Compound **7**, wherein the phenyl ring was unsubstituted, exhibited moderate activity of 31 μM. Figure 2 is a graphical summary of the anti-tubercular activity presented by the different compounds.

The molecular weight (MW), total polar surface area (tPSA), and calculated lipophilicity (ClogP) for all compounds were predicted using chemdraw, version 15. These compounds are predicted to have good drug-like properties, as they all possessed MW < 500, ClogP < 2, and a tPSA < 160.

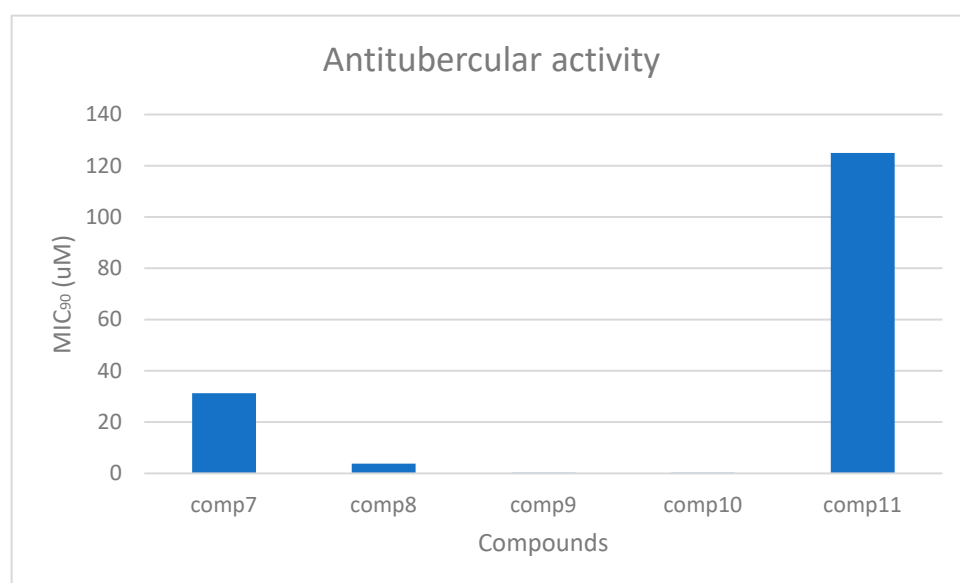


Figure 2. Bar graph presentation of antitubercular activity.

3. Materials and Methods

3.1. General Methods

Reagents and solvents were purchased from various chemical vendors, including Ambeed, AK Scientific, Rochelle, Labchem, and Merck. The progress of the reactions was monitored through the thin-layer chromatography method using Merck 60F₂₅₄ silica gel sheets supported on aluminum. UV light (254 and 366 nm) or iodine vapor staining were used to visualize the developed sheets. Melting points (m.p.) were determined with a Buchi B545 apparatus. ¹H and ¹³C nuclear magnetic resonance (NMR) spectra were acquired on a Bruker Avance III 600 spectrophotometer at 600 MHz and 151 MHz, respectively, in deuterated DMSO-*d*₆. Chemical shifts are reported in parts per million (ppm) and were referenced to the residual solvent peaks (DMSO-*d*₆): 2.50 and 39.52 ppm for ¹H and ¹³C-NMR, respectively. Spin multiplicities are given as s (singlet), d (doublet), t (triplets), m (multiplet), dt (doublet of triplets), td (triplet of doublets), and dd (doublet of doublets). Coupling constants (*J*) are reported in Hz. A Bruker micrOTOF-Q II mass spectrometer was used to record high-resolution mass spectra (HRMS) utilizing atmospheric pressure chemical ionization (APCI) in positive ion mode. A full scan from 50 to 1600 *m/z* was carried out at a capillary voltage of 4500 V, an end-plate offset of 500 V, 1.8 Bar nebulizers, and a collision cell RF voltage of 150 Vpp.

3.2. General Synthetic Procedure

The following general synthetic transformations were used to achieve the target compounds:

- (i) *N*-acylation: 2-amino-5-nitrothiazole (2.3 g, 15.9 mmol) and 2-chloroacetyl chloride (2.2 eq) were added into an ice-cold round-bottom flask containing dichloromethane (DCM) and triethylamine (TEA) (1.2 eq). The mixture was stirred at room temperature for 24–36 h. The reaction was monitored by TLC, and upon completion, the reaction mixture was concentrated in vacuo. The resulting mixture was then washed with water, filtered, washed with hexane, filtered, and dried to afford intermediate **5** in 80% yields [17].
- (ii) Intramolecular cyclization: Into a round-bottom flask, 3 g (11.4 mmol) of compound **5** was added, followed by 1.7 g (2 eq, 22.7 mmol) of ammonium thiocyanate, and 20 mL of ethanol, and the mixture was refluxed for 3–4 h. Upon reaction completion (monitored by TLC), the mixture was left to stand still at room temperature (rt) overnight. The resulting precipitate was filtered and washed with ethanol and water to obtain intermediate **6** in 74% yields [17].

(iii) Mannich base condensation: Samples of 0.3 g (1.2 mmol) of **6**, piperidine (5 eq), and appropriate benzaldehydes (5 eq) were added into a round-bottom flask containing 10 mL of ethanol, and the resultant mixture was refluxed for 24–36 h. The reaction was monitored by TLC, and after completion, it was kept at ~8 °C overnight. The resulting precipitate was then filtered, washed with water, and finally recrystallized in 1,4-dioxane to achieve the target compounds (**7–11**) in low to moderate yields.

(*E*)-2-((5-nitrothiazol-2-yl)imino)-5-(phenyl(piperidin-1-yl)methyl)thiazolidin-4-one, **7**. Yellow powder; 32% yield; mp: 210–211 °C; ¹H NMR (600 MHz, DMSO-d₆) δ 7.63–7.52 (m, 5H), 7.45 (s, 1H), 3.92 (s, 2H), 3.63 (s, 2H), 1.62–1.50 (m, 10H). ¹³C NMR (151 MHz, DMSO-d₆) δ 179.79, 173.84, 134.43, 130.13, 129.96, 129.94, 129.64, 129.35, 50.32, 49.62, 26.21, 25.59, 23.86. *m/z* HRMS (APCI) found 273.1096. Calcd for C₁₂H₂₁N₂O₂S₂: 273.1090 [M + H]⁺.

(*E*)-2-((5-nitrothiazol-2-yl)imino)-5-(piperidin-1-yl(*m*-tolyl)methyl)thiazolidin-4-one, **8**. Yellow powder; 32% yield; mp: 208 °C; ¹H NMR (600 MHz, Chloroform-d) δ 8.00 (s, 1H), 7.55–7.53 (m, 1H), 7.28–7.25 (m, 3H), 4.05–4.02 (m, 2H), 3.57–3.55 (m, 2H), 2.46 (s, 3H), 1.99–1.21 (m, 10H). ¹³C NMR (151 MHz, CDCl₃) δ 180.52, 174.95, 138.67, 133.94, 130.75, 130.33, 129.39, 129.11, 127.24, 126.17, 50.16, 49.60, 26.16, 25.45, 24.06, 19.98. *m/z* HRMS (APCI) found 287.1265. Calcd for C₁₃H₂₃N₂O₂S₂: 287.1246 [M + H]⁺.

(*E*)-5-((3-chlorophenyl)(piperidin-1-yl)methyl)-2-((5-nitrothiazol-2-yl)imino)thiazolidin-4-one, **9**. White powder; 25% yield; mp: 200–202 °C; ¹H NMR (600 MHz, DMSO-d₆) δ 7.83 (s, 1H), 7.69 (d, *J* = 6.6 Hz, 1H), 7.62 (d, *J* = 7.1 Hz, 1H), 7.52–7.46 (m, 3H), 3.98–3.91 (m, 2H), 3.62 (d, *J* = 5.4 Hz, 2H), 1.84–1.55 (m, 10H). ¹³C NMR (151 MHz, DMSO-d₆) δ 179.16, 173.67, 134.59, 133.00, 132.63, 131.56, 130.65, 129.13, 128.41, 125.04, 50.48, 49.79, 26.22, 25.60, 23.82. *m/z* HRMS (APCI) found 307.0708. Calcd for C₁₂H₂₀ClN₂O₂S₂: 307.0700 [M + H]⁺.

(*E*)-5-((3-methoxyphenyl)(piperidin-1-yl)methyl)-2-((5-nitrothiazol-2-yl)imino)thiazolidin-4-one, **10**. Off white powder; 30% yield; mp: 130–132 °C; ¹H NMR (600 MHz, DMSO-d₆) δ 7.61 (s, 1H), 7.43 (t, *J* = 8.0 Hz, 1H), 7.23–7.20 (m, 1H), 7.18–7.17 (m, 1H), 7.03 (d, *J* = 10.2 Hz, 1H), 3.97–3.91 (m, 2H), 3.82 (s, 3H), 3.64–3.63 (m, 2H), 2.11–1.04 (m, 10H). ¹³C NMR (151 MHz, DMSO-d₆) δ 179.71, 173.78, 160.15, 135.83, 130.69, 129.89, 129.65, 122.01, 115.86, 115.41, 55.75, 50.31, 49.61, 26.22, 25.58, 23.85. *m/z* HRMS (APCI) found 307.0709. Calcd for C₁₂H₂₀ClN₂O₂S₂: 307.0700 [M + H]⁺.

((*E*)-5-((2-chlorophenyl)(piperidin-1-yl)methyl)-2-((5-nitrothiazol-2-yl)imino)thiazolidin-4-one, **11**. Brown powder; 23% yield; mp: 201–202 °C; ¹H NMR (600 MHz, DMSO-d₆) δ 7.82 (s, 1H), 7.68 (dd, *J* = 7.7, 1.6 Hz, 1H), 7.61 (dd, *J* = 7.9, 1.3 Hz, 1H), 7.52–7.44 (m, 3H), 3.92–3.91 (m, 2H), 3.61–3.60 (m, 1H), 1.87–1.26 (m, 10H). ¹³C NMR (151 MHz, DMSO-d₆) δ 183.94, 178.44, 139.36, 137.77, 137.40, 136.34, 135.42, 133.90, 133.18, 129.81, 55.24, 54.55, 30.97, 30.36, 28.57. *m/z* HRMS (APCI) found 303.1208. Calcd for C₁₃H₂₃N₂O₂S₂: 303.1195 [M + H]⁺.

3.3. In Vitro Antitubercular Evaluation

The antitubercular property of the target compounds was established using the previously reported methods [18]. A 10 mL culture of the *gfp* reporter *Mtb* strain was grown to an optical density (OD₆₀₀) of 0.6–0.7 in Middlebrook 7H9 media, which was supplemented with 0.03% casitone (CAS), 0.4% glucose, and 0.05% tyloxapol. Fifty (50) mL of *Mtb*-containing medium was introduced to each well of a 96-well plate, followed by the addition of target compounds at a concentration range between 0.244 and 125 μM. The plates were sealed and incubated at 37 °C with 5% CO₂ and humidification. Rifampicin (RIF) (MIC₉₀) and 5% DMSO were used as the minimum and maximum growth controls, respectively. On day 14 following incubation, fluorescence readings were recorded for each well at 485 and 520 nm using a plate reader (FLUOstar OPTIMA, BMG LABTECH). These readings were standardized and used to generate dose–response curves from which the minimal inhibitory concentration (MIC₉₀) was estimated using the Levenberg–Marquardt damped least-squares (DLS) method, and it was found that the lowest concentration inhibited the growth of more than 90% of the bacterial population [19,20].

3.4. In Vitro Cell Toxicity Evaluation

Overt cell toxicity potential was established as previously reported. Manually counted HEK-293 cells were plated in 384-well plates at a density of 5×10^3 cells and a volume of 50 μ L per well. The cells were cultured using Dulbecco's Modified Eagle Medium (DMEM) containing 10% fetal bovine serum (FBS). Compounds at 32 μ g/mL were added to each well, and the plates were incubated for 20 h at 37 °C in 5% CO₂. This was followed by the addition of resazurin (5 μ L) and incubation for 3 more hours. The fluorescence of each well was measured using a Tecan M1000 Pro monochromator plate reader at 590 nm. The fluorescence readings, along with the concentrations of the compounds, was used to generate the CC₅₀ (concentration required to inhibit 50% cell growth) values [21].

4. Conclusions

In this study, five Mannich base nitrothiazole derivatives were synthesized, characterized, and evaluated in vitro against Mtb, fungi, and Gram-negative and -positive bacteria, as well as against normal human cell lines. Four compounds exhibited selective antitubercular activity in the range of <0.244–31.25 μ M, with compounds **9** and **10** being the most (<0.244 μ M) active. These compounds had no activity against human cell line, and hence are likely to be non-toxic to humans. In addition, the compounds followed the Lipinski rule of five, having molecular weights below 500 Da and ClogP values of less than 5. They also had total polar surface areas less than 160. Thus, there is still room for further exploration. This study highlights Mannich base nitrothiazole derivatives as a viable source of novel drugs in the fight against TB.

Supplementary Materials: The following supporting information can be downloaded at: Scheme S1: Structures of fragments formed during ionization; Figure S1: ¹H NMR spectrum of compound **7**; Figure S2: ¹³C NMR spectrum of compound **7**; Figure S3: HRMS of compound **7**; Figure S4: ¹H NMR spectrum of compound **8**; Figure S5: ¹³C NMR spectrum of compound **8**; Figure S6: HRMS of compound **8**; Figure S7: ¹H NMR spectrum of compound **9**; Figure S8: ¹³C NMR spectrum of compound **9**; Figure S9: HRMS of compound **9**; Figure S10: ¹H NMR spectrum of compound **10**; Figure S11: ¹³C NMR spectrum of compound **10**; Figure S12: HRMS of compound **10**; Figure S13: ¹H NMR spectrum of compound **11**; Figure S14: ¹³C NMR spectrum of compound **11**; Figure S15: HRMS of compound **11**.

Author Contributions: Conceptualization, P.S.D.; methodology, D.H. and A.J.; validation, D.F.W.; formal analysis, P.S.D.; investigation, P.S.D.; resources, R.M.B. and L.J.L.; data curation, P.S.D.; writing—original draft preparation, P.S.D.; writing—review and editing, P.S.D. and R.M.B.; supervision, R.M.B. and L.J.L.; project administration, R.M.B.; funding acquisition, R.M.B. All authors have read and agreed to the published version of the manuscript.

Funding: This project received financial support from the National Research Foundation (NRF) Research Grant (grant no: 137776) awarded to R.M.B. The antimicrobial and cell toxicity evaluation performed by CO-ADD (The Community for Antimicrobial Drug Discovery) was funded by the Wellcome Trust (UK) and The University of Queensland (Australia).

Data Availability Statement: The ¹H and ¹³C spectral data for each target compound and APCI-HRMS are available in the Supplementary Materials.

Acknowledgments: This project received financial support from the National Research Foundation (NRF) Research Grant (grant no: 137776) awarded to R.M.B. The antimicrobial and cell toxicity evaluation performed by CO-ADD (The Community for Antimicrobial Drug Discovery) was funded by the Wellcome Trust (UK) and The University of Queensland (Australia). The NMR spectra were recorded by Otto Daniel and Johan Jordaan of the SASOL Centre for Chemistry, North-West University. The authors acknowledge the South African Medical Research Council (SHIP grant to D.F.W.) for their financial support toward antitubercular evaluation. The authors appreciate the financial and infrastructural support from North-West University, Potchefstroom campus.

Conflicts of Interest: The authors declare no conflicts of interest.

References

1. WHO. *Global Tuberculosis Report 2018*; World Health Organization: Geneva, Switzerland, 2018.
2. Lam, K.K.; Zheng, X.; Forestieri, R.; Balgi, A.; Nodwell, M.; Vollett, S.; Anderson, H.; Andersen, R.; Av-Gay, Y.; Roberge, M. Nitazoxanide stimulates autophagy and inhibits mTORC1 signaling and intracellular proliferation of *Mycobacterium tuberculosis*. *PLoS Pathog.* **2012**, *8*, e1002691. [CrossRef] [PubMed]
3. Gengenbacher, M.; Kaufmann, S.H. *Mycobacterium tuberculosis*: Success through dormancy. *FEMS Microbiol. Rev.* **2012**, *36*, 514–532. [CrossRef] [PubMed]
4. Dietrich, J.; Doherty, T.M. Interaction of *Mycobacterium tuberculosis* with the host: Consequences for vaccine development. *APMIS* **2009**, *117*, 440–457. [CrossRef] [PubMed]
5. Raffetseder, J.; Pienaar, E.; Blomgran, R.; Eklund, D.; Brodin, V.P.; Andersson, H.; Welin, A.; Lerm, M. Replication rates of *Mycobacterium tuberculosis* in human macrophages do not correlate with mycobacterial antibiotic susceptibility. *PLoS ONE* **2014**, *9*, e112426. [CrossRef] [PubMed]
6. Connolly, L.E.; Edelman, P.H.; Ramakrishnan, L. Why is long-term therapy required to cure tuberculosis? *PLoS Med.* **2007**, *4*, e120. [CrossRef] [PubMed]
7. Riccardi, G.; Pasca, M.R.; Chiarelli, L.R.; Manina, G.; Mattevi, A.; Binda, C. The DprE1 enzyme, one of the most vulnerable targets of *Mycobacterium tuberculosis*. *Appl. Microbiol. Biotechnol.* **2013**, *97*, 8841–8848. [CrossRef] [PubMed]
8. WHO. *Global Tuberculosis Report 2022*. Available online: <https://www.who.int/publications/i/item/9789240061729> (accessed on 6 March 2024).
9. Peddireddy, V.; Doddam, S.N.; Ahmed, N. Mycobacterial dormancy systems and host responses in tuberculosis. *Front. Immunol.* **2017**, *8*, 84. [CrossRef] [PubMed]
10. Iacobino, A.; Piccaro, G.; Giannoni, F.; Mustazzolu, A.; Fattorinia, A. *Mycobacterium tuberculosis* is selectively killed by rifampin and rifapentine in hypoxia at neutral pH. *Antimicrob. Agents Chemother.* **2017**, *61*, e02296-16. [CrossRef] [PubMed]
11. Yu, X.; Li, C.; Hong, W.; Pan, W.; Xie, J. Autophagy during *Mycobacterium tuberculosis* infection and implications for future tuberculosis medications. *Cell. Signal.* **2013**, *25*, 1272–1278. [CrossRef] [PubMed]
12. Kumar, G.; Kapoor, S. Targeting mycobacterial membranes and membrane proteins: Progress and limitations. *Bioorg. Med. Chem. Lett.* **2023**, *81*, 117212. [CrossRef] [PubMed]
13. Iacobino, A.; Piccaro, G.; Giannoni, F.; Mustazzolu, A.; Fattorini, L. Activity of drugs against dormant *Mycobacterium tuberculosis*. *Int. J. Mycobacteriol.* **2016**, *5*, 94. [CrossRef] [PubMed]
14. Novoa-Aponte, L.; Ospina, C.Y. *Mycobacterium tuberculosis* P-type ATPases: Possible targets for drug or vaccine development. *Biomed. Res. Int.* **2014**, *2014*, 296986. [CrossRef] [PubMed]
15. Dartois, V.A.; Rubin, E.J. Anti-tuberculosis treatment strategies and drug development: Challenges and priorities. *Nat. Rev. Microbiol.* **2022**, *20*, 685–701. [CrossRef] [PubMed]
16. Odingo, J.; Bailey, M.A.; Files, M.; Early, J.V.; Alling, T.; Dennison, D.; Bowman, J.; Dalai, S.; Kumar, N.; Cramer, J.; et al. In Vitro Evaluation of Novel Nitazoxanide Derivatives against *Mycobacterium tuberculosis*. *ACS Omega* **2017**, *2*, 5873–5890. [CrossRef] [PubMed]
17. Hart, D.; Legoabe, L.J.; Jesumoroti, O.J.; Jordaan, A.; Warner, D.F.; Steventon, R.; Beteck, R.M. Nitrothiazole-thiazolidinone hybrids: Synthesis and in vitro antimicrobial evaluation. *Chem. Biodivers.* **2022**, *19*, e202200729. [CrossRef] [PubMed]
18. Beteck, R.M.; Jordaan, A.; Seldon, R.; Laming, D.; Hoppe, H.C.; Warner, D.F.; Khanye, S.D. Easy-To-Access Quinolone Derivatives Exhibiting Antibacterial and Anti-Parasitic Activities. *Molecules* **2021**, *26*, 1141. [CrossRef] [PubMed]
19. Dube, P.S.; Legoabe, L.J.; Jordaan, A.; Jesumoroti, O.J.; Tshiwawa, T.; Warner, D.F.; Beteck, R.M. Easily accessed nitroquinolones exhibiting potent and selective anti-tubercular activity. *Eur. J. Med. Chem.* **2021**, *213*, 113207. [CrossRef] [PubMed]
20. Du Preez, C.; Legoabe, L.J.; Jordaan, A.; Jesumoroti, O.J.; Warner, D.F.; Beteck, R.M. Arylnitro monocarbonyl curcumin analogues: Synthesis and in vitro antitubercular evaluation. *Chem. Biol. Drug Des.* **2023**, *101*, 717–726. [CrossRef] [PubMed]
21. Blaskovich, M.A.; Zuegg, J.; Elliott, A.G.; Cooper, M.A. Helping Chemists Discover New Antibiotics. *ACS Infect. Dis.* **2015**, *1*, 285–287. [CrossRef] [PubMed]

Disclaimer/Publisher's Note: The statements, opinions and data contained in all publications are solely those of the individual author(s) and contributor(s) and not of MDPI and/or the editor(s). MDPI and/or the editor(s) disclaim responsibility for any injury to people or property resulting from any ideas, methods, instructions or products referred to in the content.